

Molecular interactions: nanocalorimetry of DNA molecules

Biomolecular Interactions : methods and applications
Johannes Geiselmann - Hervé Guillou

Karina DAMBERG
Anass ESSENNI
Aida Gabriela FERNANDEZ CONTRERAS
Matteo MARENGO
Daniel de Jesus PLIEGO SOSA



PHELMA - Grenoble INP - 3A BIOMED
UGA - Master Nanobiotechnology
CNRS - Institut Louis Néel
November 28th, 2022

Molecular interactions: nanocalorimetry of DNA molecules

PHELMA - Grenoble INP // Université Grenoble Alpes

Abstract

Hybridization of DNA strands is a subject that is thoroughly studied in biology. Therefore, it is important to understand its mechanism and the different thermodynamic parameters involved. To address these questions, calorimetry experiments were performed. However, to change from the canonical duplex, nanostructures such as the loop formed with two strands were studied. The first one was differential scanning calorimetry (DSC) where the sample and a reference buffer are maintained at the same temperature throughout the experiment. The compensation power to keep these two vials at the same temperature is measured as a function of temperature. The second method used was isothermal titration calorimetry (ITC), where injections of the ligand triggers a reaction in the sample cell, and the resulting heat difference necessary to maintain the cells at a constant temperature is calculated. The different thermodynamic models that were extracted from these experiments (molar enthalpy, molar entropy) correspond to the ones that can be predicted using numerical models such as Nupack or Dinamelt. It proves that hybridization is a complex process that involves many parameters that have to be carefully tuned in order to get the expected DNA structure.

Keywords: Hybridization, Differential Scanning Calorimetry, Isothermal titration calorimetry, Nupack model, Dinamelt model, Dissociation constant

1 Introduction

The objective of this study is to investigate the thermodynamics of the hybridization of DNA. DNA Hybridization is the process in which two complementary single-stranded DNA interact via non-covalent bonds to form a double-stranded molecule [1]. However, in the present work not the canonical duplex, but other DNA structures such as the **Holliday Junction** (an assembly of four DNA strands), and the **loop Structure** made of two DNA strands are studied.

1.1 Holliday Junctions: Biological Functions

Holliday Junctions are DNA nanostructures composed of four double-stranded DNA that interact together. They adopt a specific conformational structure that is shown in Fig. 1 and Fig. 2.

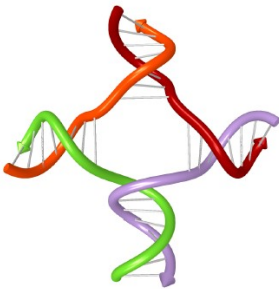


Figure 1: Cartoon representation of the Holliday Junction where the helical structure is well observed. Adapted from [2].

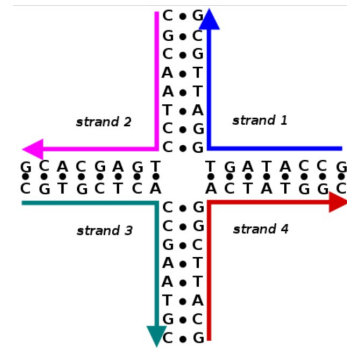


Figure 2: Schematic of a Holliday Junction showing the complementarity of base sequences. Adapted from [3].

ST1: CGCAATCCTGAGCACG

ST2: CGTGCTCACCGAATGC

ST3: GCATTCCGACTATGGC

ST4: GCCATAGTGGATTGCG

Figure 3: Set of sequences used to form the Holliday Junction. Adapted from [2].

The set of sequences shown in Fig. 3 was used for the experimental section.

Holliday Junctions (HJ) have many biological functions. One of them is acting as an intermediary in many recombination processes (exchange of genetic material between different organisms) that ultimately increases genetic diversity by shifting genes between two chromosomes [4] and helps with the repair of double-stranded DNA. The HJ is the substrate of recombination enzymes that promote branch migration [5] and can also relieve helical strain in

DNA sequences [6].

1.2 DNA Origami and Loop Structures

DNA nanotechnology is the design of complex DNA structures with branched oligonucleotides as a basic component. One common motif found in these structures is the double crossover complex. It contains two HJ in proximity to each other [3] and is shown in Fig. 4.



Figure 4: Double-Crossover complex. Adapted from [3].

This complex is of outmost importance as it is the first scaffold used in DNA Origami. DNA Origami is the formation of complex DNA shapes at the nanoscale using folded DNA strands. It has found diverse applications in areas like molecular analysis, drug delivery, and biosensing [7].

The second structure that was studied is the loop structure. It is a structure formed by two strands with partial complementary [2]. The structure is shown in Fig. 5.



Figure 5: Loop-structure. Adapted from [2].

The Loop forming sequences analyzed in this work are shown in Fig. 6

LOOPSTP1: GCTTCTATTGACATGCCACCGTGCTTAGAGTG
LOOPSTP2: CACTCTAAGCACGGTGGCATGTCAATAGAAGC
LOOPSTP2L4: CACTCTAAGCACGGTGTTTTTGCATGTCAATAGAAGC
LOOPSTP2L8: CACTCTAAGCACGGTGTTTTTGTGCATGTCAATAGAAGC
LOOPSTP2L16: CACTCTAAGCACGGTGTTTTTGTGCATGTCAATAGAAGC
LOOPSTP2L32: CACTCTAAGCACGGT(T)₃₂GCATGTCAATAGAAGC
LOOPSTP2L64: CACTCTAAGCACGGT(T)₆₄GCATGTCAATAGAAGC

Figure 6: Set of sequences used for the Loop Structure. Adapted from [2].

1.3 Sequences of our group

We are the group from the 28/11/2022. As the first four groups studied LOOPSTP2L4 and LOOPSTP2L8, we decided to study the **LOOPSTP2L16** and **1PTSPOOL** as the complementary sequence.

- **1PTSPOOL** : CACCGTGCTTAGAGTG GCTTC-TATTGACATGC
- **LOOPSTP2L16** : CACTCTAAGCACGGTGTTTTT TTTTTTTTTTTT**T**GCATGT**CA**ATAGAAGC

1.4 Predictions of thermodynamic models

Some models easily available on the internet can either predict the thermodynamic parameters or the final shape of the two hybridized DNA strands. These softwares include **Nupack** and **MFold** or **Dinamelt**.

1.4.1 Nupack

The first model that was used was Nupack. [8]. We proceeded with the desired concentration of 50 μ M. The set-up is observed in Fig. 7.

Figure 7: Parameters in the input to do the theoretical analysis on Nupack with LOOPSTP2L16 and 1PTSPOOL. Adapted from [8].

The model that was obtained after that analysis is shown in Fig. 8.

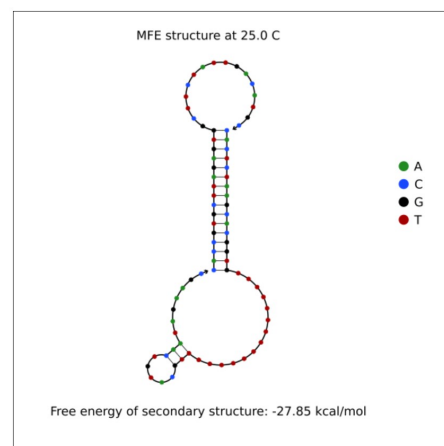


Figure 8: Model found by the Nupack software with the Loop structure. Adapted from [8].

This model has indeed a loop structure, and it shows the complementarity that was identified between the sequences, so it can first be argued that Nupack manages to find the structure.

1.4.2 Dinamelt

Dinamelt [9] is another software that is used to model the hybridization of two different strands of DNA and RNA. Once again, the base sequences is be inserted as well as their ideal concentrations (50 μ M. The set-up of the software is the one in Fig. 9.

Hybridization of two Different Strands of DNA or RNA

Do you only have one sequence? Use [this form](#). Use [advanced form](#)

Job Name: Hybridization Modeling

Sequence 1: 5' - 3'

Rev. Comp. ☐

Sequence 2: 5' - 3'

Temperature range: From °C by °C to °C

NA type: ☒ DNA ☐ ORNA ☐ ORNA2

Initial concentrations: [A₀]: [B₀]: Units:

Figure 9: The Dinamelt set-up with the ideal concentrations. Adapted from [9].

This software is really powerful as we can obtain the Heat capacity plot in Fig. 10.

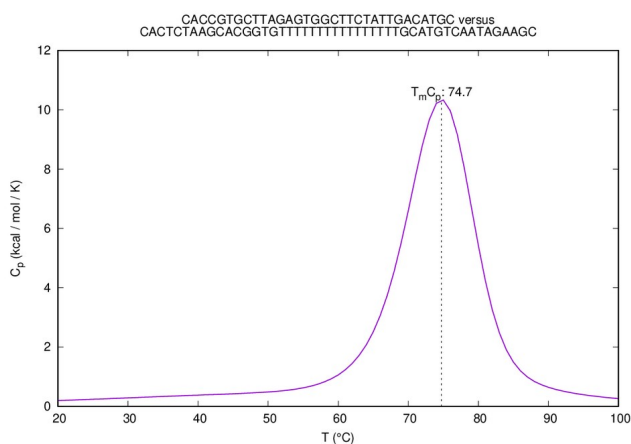


Figure 10: Heat Capacity Plot with the ideal concentrations of Seq. A and Seq. B. Adapted from [9].

After getting an overlook from these models, we can obtain and analyze experimental data based on calorimetry to compare and determine the accuracy of these programs for predicting theoretical models.

2 Experimental method

2.1 Preparation of the solutions

As mentioned before, it was decided to study the hybridization of LOOPSTP2L16 with 1PTSPPOOL by differential scanning calorimetry (DSC) and isothermal titration calorimetry (ITC). For this, it was initially intended to prepare 350 μL of both LOOPSTP2L16 and 1PTSPPOOL solutions 80 μM for DSC as well as 1500 μL of 1PTSPPOOL 12 μM and 400 μL of LOOPSTP2L16 80 μM for ITC. The concentration of the solutions was assessed with a spectrophotometer. From the measurements it was determined that the concentration was different than the intended, and therefore, dilutions were made to balance the concentration of the solutions. For DSC for example, instead of 80 μM , 47.8 μM and 51.2 μM of 1PTSPPOOL and LOOPSTP2L16

respectively were used, since there was not enough left of the concentrated solution. The final concentrations obtained were:

- 1PTSPPOOL DSC : 47.8 μM
- LOOPSTP2L16 DSC : 51.2 μM
- 1PTSPPOOL ITC : 10.1 μM
- LOOPSTP2L16 ITC : 63.3 μM

2.2 Introduction to calorimetry

Most biochemical reactions are accompanied by the release or absorption of heat. Therefore, calorimetry is a method to quantify the progress of a reaction. There are three methods to measure the heat exchanged during the reaction [7].

- Measuring the temperature change due to the reaction. (If the measured temperature change is multiplied by the heat capacity, it gives the heat of the reaction.
- Power compensation: the power consumption of the heater is measured as a function of time.
- Heat conduction: For this, constant temperature is passively maintained.

2.3 Differential Scanning calorimetry

Differential Scanning calorimetry is a technique in which the difference in the amount of heat required to increase the temperature of a sample and reference is measured as a function of temperature [10]. There are different types of DSC; Heat-flux DSC, Power differential DSC and Fast-scan DSC.

2.3.1 Heat-flux DSC

Heat-flux Differential scanning calorimetry (DSC) has the set-up shown in Fig 11.

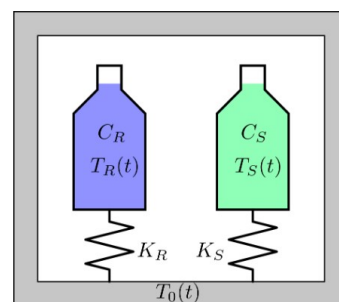


Figure 11: Experimental set-up for the DSC measurement. The blue vessel is the reference vessel. The green vessel is the sample vessel. The temperature of the furnace is $T_0(t)$. Adapted from [11].

We have two cells : a reference cell filled with a reference sample (often water or a buffer) and a cell filled with the sample of interest [11]. We do not inject any more sample during the experiment. The reference sample does not have any phase transformation.

The furnace temperature is T_0 and is ramped up or down with the rate $\gamma = \frac{dT_0}{dt}$. The temperature is scanned with a defined rate constant. The reaction occurs in the sample cell, and it releases energy if it is exothermic or absorbs energy if it is endothermic.

During a scan-up, the temperature increases linearly. The reference side generally heats up faster than the sample side during the heating of the DSC measuring cell due to the heat capacity C_p [12]. It is shown in Fig 12.

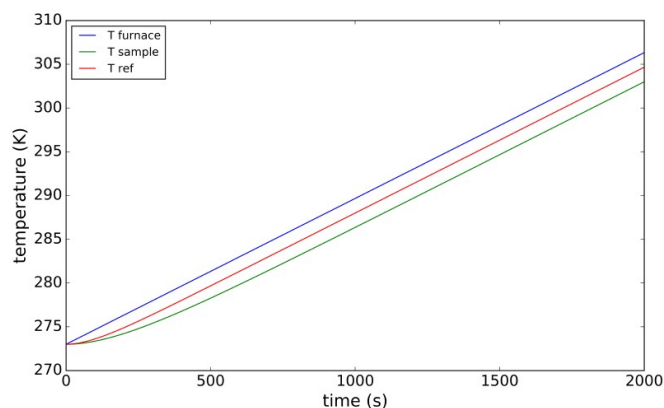


Figure 12: Linear variations of temperature after the temperature is increased.

Then, when the reaction occurs there is no parallel behavior anymore.

2.3.2 Power compensation calorimetry

The Power compensation DSC has the set-up of Fig 13.

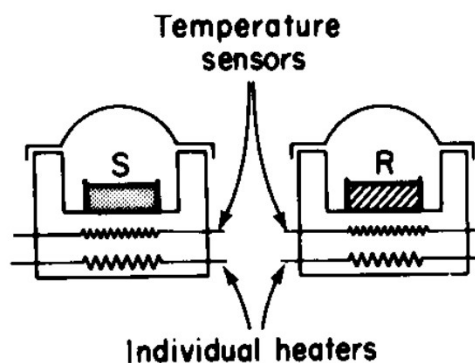


Figure 13: Experimental set-up for the Power compensation DSC measurement. S is the sample and R is the reference. Adapted from [13].

In Power-compensation DSC, the temperatures of the sample and reference are controlled independently using separate, identical furnaces. The temperatures of the sample and reference will be identical thanks to the power compensation. The energy required to do that action is a measure of the enthalpy and heat capacity change [13].

2.4 Isothermal titration calorimetry

Isothermal scanning calorimetry (ITC) has a different principle than DSC. For ITC, the ligand solution is progressively injected into the sample cell and the difference

of heat is calculated from the power needed to keep sample and reference cells at the same temperature [7]. The basic set-up of this experiment is shown in Fig 14.

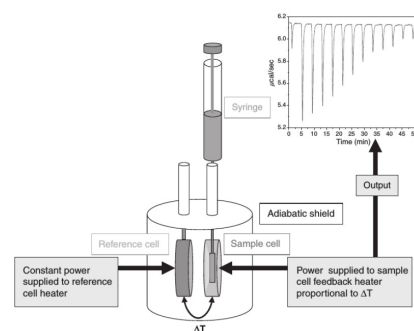


Figure 14: ITC set-up. The difference of power consumption of the heaters of the sample and reference cells are used to calculate the heat produced by the reaction. Adapted from [7].

When raw data is plotted, the behavior observed is the one of Fig 15 with the amount of power delivered that decreases after each injection until it reaches saturation at the end.

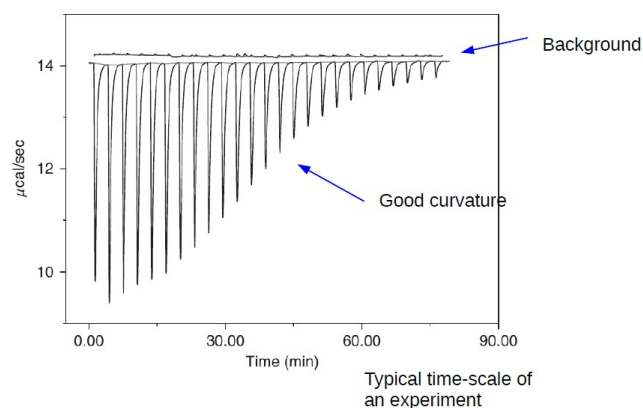


Figure 15: ITC classical curve. Adapted from [7].

In an exothermic reaction, the temperature in the sample cell increases when we add ligand. Therefore, the feedback power is decreased. Observations are plotted as the power needed to maintain the reference and the sample cell at an identical temperature against time. Every spike corresponding to one ligand injection is integrated with respect to time to have the total heat exchanged. These heat effects are regarded in respect to the molar ratio [14]. Fig 16 is a sum-up of what is said.

ITC and DSC can be used as complementary techniques to overcome some of their limitations. While DSC is a routine technique with high sensitivity, it shows limitations, including reduced sample size as well as its dynamic nature, for certain applications, because it implies a “lack of equilibrium” conditions whereas the properties to be determined are equilibrium properties [15]. ITC, on the other hand, allows analysis at a defined temperature, while thermal melting approaches provide thermodynamic information specific to the melting temperature [16]. However, it can suffer from drifts, has a limited range for consistently measured bind-

ing affinities and also, since heat is a universal signal with contribution from multiple processes, it can be complicated to determine the contribution because of binding [17].

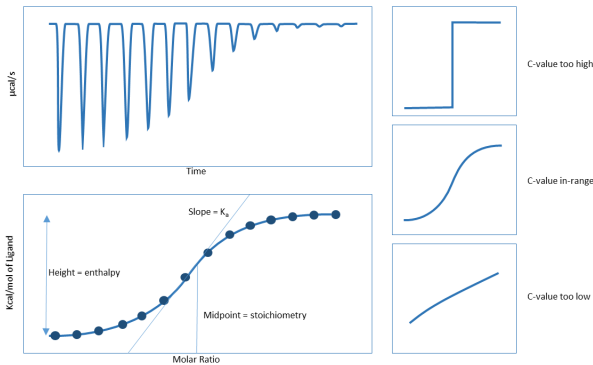


Figure 16: ITC thermogram, Data that will be measured. Adapted from [14].

3 Experimental analysis of real DSC data

3.1 28/11/2022 DSC Analysis

To plot the different graphs based on the experiment results and analyze the thermodynamics of the reaction, python scripts were given [2].

First, the raw data for the 28/11/2022 experiment was plotted with the two first scans up and the two first scans down. Results in Fig 17 were obtained.

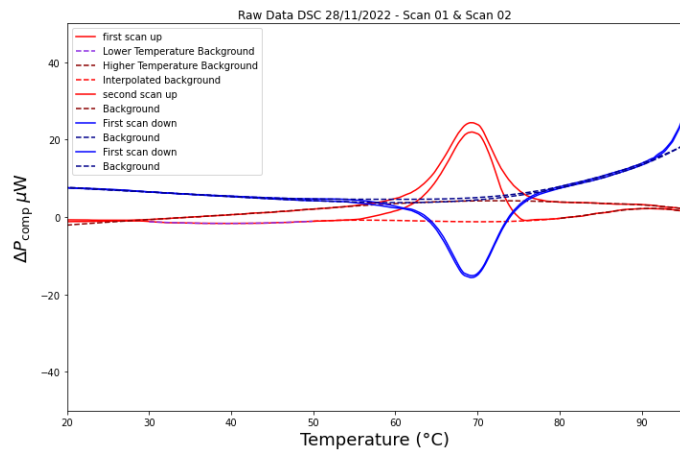


Figure 17: Raw Data of scan 01 and scan 02 - 28/11/2022

In this curve, we observe that the reaction from the sample should appear around 70°C. The first and second scans validate this observation. A behavior that is a bit strange is with the scan down. Indeed, the scan down has a higher ΔP_{comp} than the scan up (we have 8 μW at 20°C instead of 0 μW with the scan up. Another thing to note is that the first scan up does not overlap perfectly with the second scan up even though they are very similar. Concerning the background power, its plot corresponds to what we were expecting, the limits are used to fit the background (in our

case with polynomial function). We plot other scans in Fig 18 to look whether the behavior is the same.

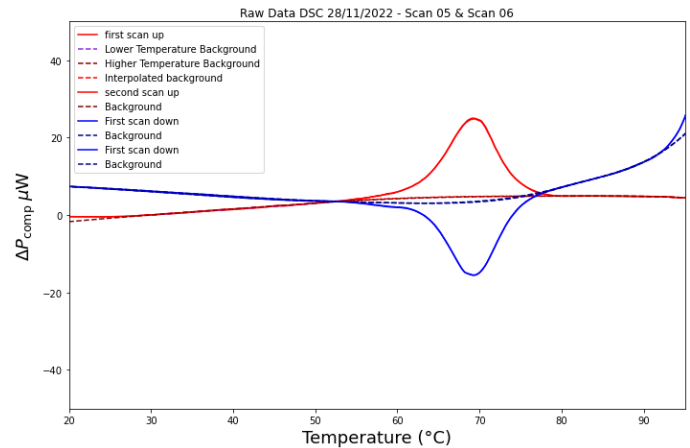


Figure 18: Raw Data of scan 05 and scan 06 - 28/11/2022

With these scans, we observe the same behavior as with scans one and two. In contrast with the two scans up in Fig 17, here we observe that two scans up fit perfectly with each other. This suggests that basing the analysis on the first scans of the experiment might not be the best idea since the behavior seen suggests a sort of latency in the experiment for the measurements to be totally stable and suitable for analysis.

After the raw data plot, another variable that can be computed is the molar heat compensation. The formula that will be used is detailed underneath.

$$\Delta C_p = \frac{P_{comp} - P_{background}}{\gamma \times V_0 \times C_0} \quad (1)$$

- P_{comp} is the measured raw data
- $P_{background}$ is the determined background
- γ is the scan rate (1/60 K/s)
- $V_0 = 300\mu L$ is the sample volume
- C_0 is the experimental double strand concentration

Its evolution along the temperature can be observed in Fig 19.

On this graph again, it is observed that the reaction should occur around 70°C.

The final data that was calculated to analyze the results given by DSC is the molar enthalpy and the molar entropy.

$$\Delta H = \int_{T_{min}}^{T_{max}} \Delta C_p dT \quad (2)$$

$$\Delta S = \int_{T_{min}}^{T_{max}} \frac{\Delta C_p}{T} dT \quad (3)$$

These are plotted on Fig 20 and Fig 21 respectively.

It is observed on these graphs that enthalpy and entropy surge rapidly around 70°C. It can be concluded that the four graphs (raw data, molar heat capacity, molar enthalpy and molar entropy) converge towards the same trend.

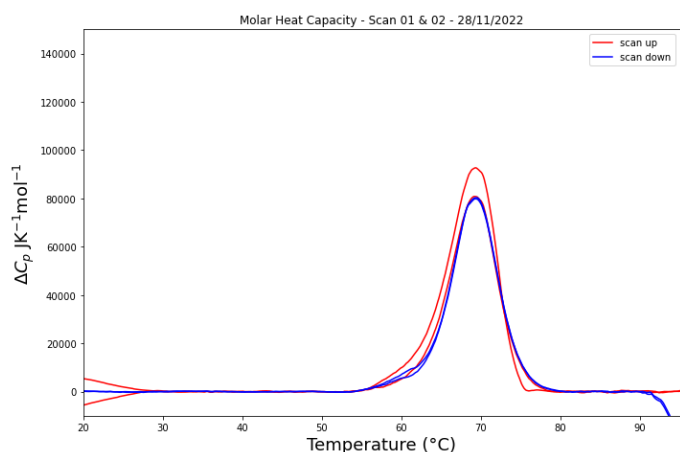


Figure 19: Molar Heat capacity scan 01 and scan 02 - 28/11/2022

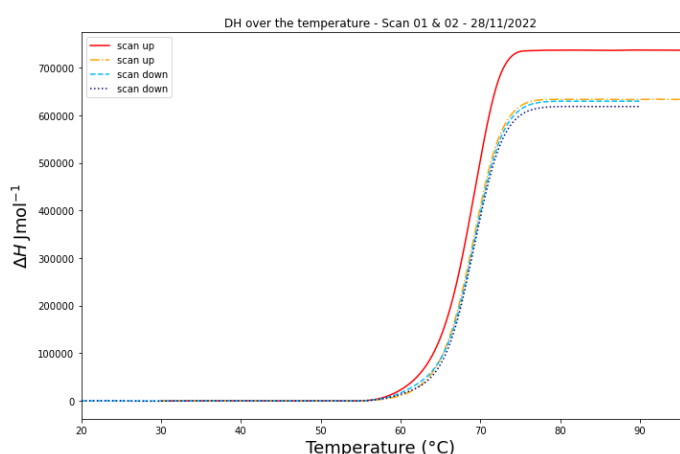


Figure 20: Molar enthalpy scan 01 and scan 02 - 28/11/2022. $\Delta H = 650000 \text{ J/mol}$ or $\Delta H = 155 \text{ kcal/mol}$.

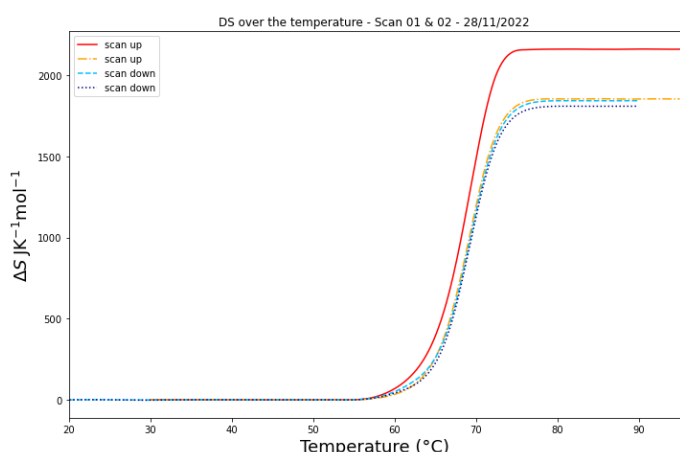


Figure 21: Molar entropy scan 01 and scan 02 - 28/11/2022. $\Delta S = 2000 \text{ J/K.mol}$ or $\Delta S = 478 \text{ cal/K.mol}$

3.2 Other groups DSC Analysis

In this part, the results obtained by the group that did the lab-work on the 14/11/2022 will be analyzed. This will be useful to compare with the results presented in the last section. To do so, the data is be analyzed in the same way as for the data of 28/11/2022. While 1PTSPPOOL was

used on both dates, for the experiment on the 14/11/2022, STP2LOOP4 was used instead of STP2LOOP16 using concentrations:

- 1PTSPPOOL DSC : 63.84 μM
- LOOPSTP2L4 DSC : 66.65 μM
- 1PTSPPOOL ITC : 7.59 μM
- LOOPSTP2L4 ITC : 55.61 μM

The raw data plot of the first two scans up and down are shown in Fig 22.

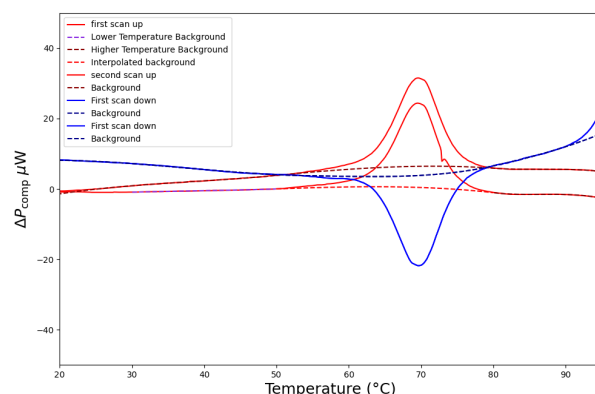


Figure 22: Raw Data of scan 01 and scan 02 - 14/11/2022

As shown before, the first and second scans also confirm that the reaction from the sample appears around 70°C. In general, in comparison with the data shown in Fig 17, the behavior is very similar and the same analysis can be applied to these curves. Note that the same inconsistency is observed between the first and second scan up. However, a small irregularity can be seen around 73°C in Fig 22 on the scan up where the graph is not as smooth as the one shown before in Fig 17. Another remarkable discrepancy can be seen at high temperatures (above 90°C) in Fig 22, where the first and second scans up have a difference of about 10 μW , in contrast with Fig 17 where the difference does not exceed 1 μW . The raw data of the last two scans (up and down) of the experiment are plotted in Fig 23.

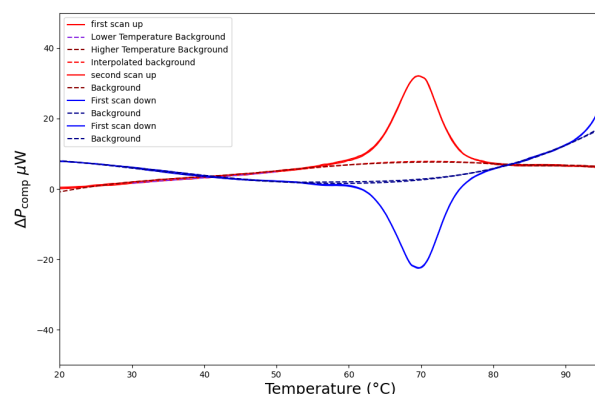


Figure 23: Raw Data of scan 03 and scan 04 - 14/11/2022

The curves are very similar and fit nicely with the ones in the section before. To conclude on the first comparison of the raw data, the results and conclusions can be confirmed by the two sets of data (data from 14/11/2022 and from 28/11/2022) since the behavior is similar and seems to be repeatedly giving the same results.

Here, the molar heat capacity, molar enthalpy and molar entropy of the 14/11/2022 data are shown in Fig 24, Fig 25 and Fig 26 respectively.

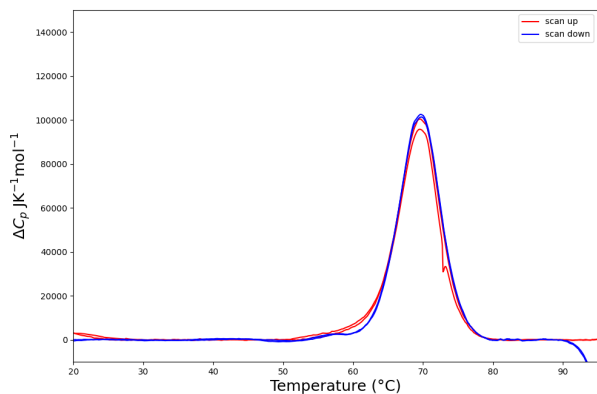


Figure 24: Molar heat capacity of scan 01 and scan 02 - 14/11/2022

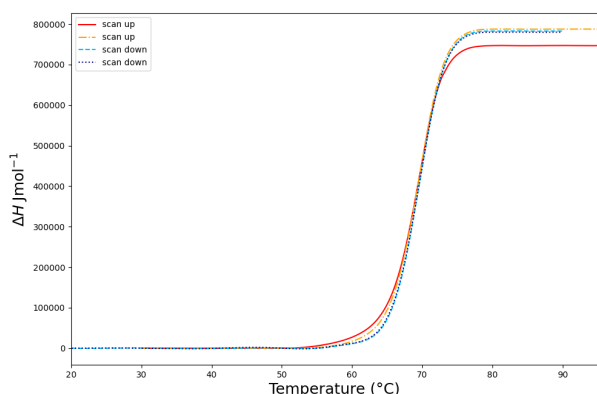


Figure 25: Molar enthalpy of scan 01 and scan 02 - 14/11/2022

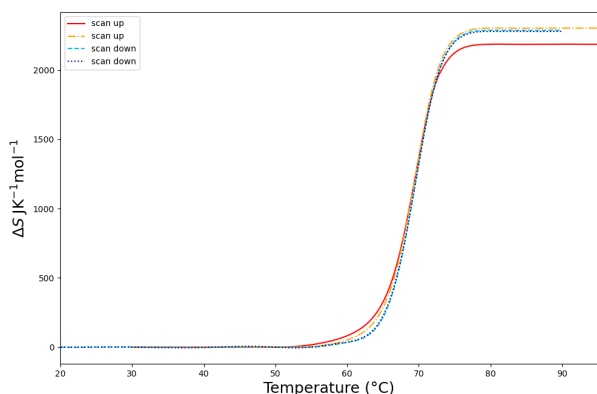


Figure 26: Molar entropy of scan 01 and scan 02 - 14/11/2022

4 Comparison with models

4.1 Mfold and Dinamelt web server

4.1.1 28/11/2022 experiments

We modeled the thermodynamic behavior of our Differential scanning calorimetry with our LOOPSTP2L16 as strand 1 and 1PTSPOOL as strand 2. The calculated concentrations for the DSC and the influence of salts, 50 mM Na⁺ and 10 mM Mg⁺⁺ is be used. The curve for the molar heat capacity is in Fig 27.

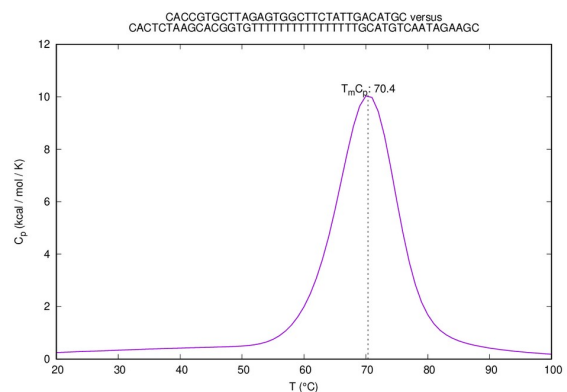


Figure 27: Mfold modeling with the calculated concentrations and the concentration of the buffer 1PTSPOOL and LOOP16.

The melting temperature is $T_m = 70.4^\circ\text{C}$ close to the found one in 19. Furthermore, $\Delta H = 151.0 \text{ kcal/mol}$ and $\Delta S = 443.4 \text{ cal/mol/K}$. It is in the same range as the one found for in Fig 20 and 21.

4.1.2 14/11/2022 experiments

We can also compare our results with the ones of 14/11/2022. On that day, the concentrations for DSC were:

- 1PTSPOOL : 63.84 μM
- LOOPSTP2L4 : 66.65 μM

The curve for the molar heat capacity is in Fig 28.

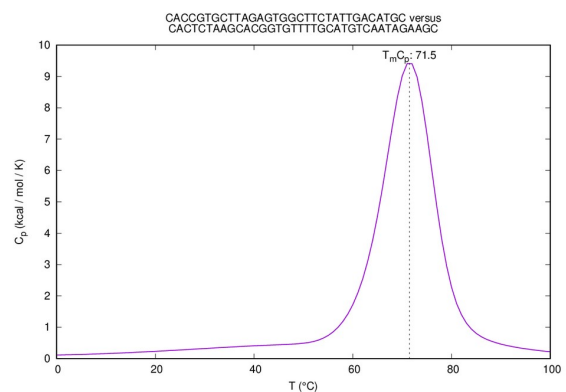


Figure 28: Mfold modeling with the calculated concentrations and the concentration of the buffer 1PTSPOOL and LOOP4.

The calculated concentrations for the DSC and the influence of salts, 50 mM Na⁺ and 10 mM Mg⁺⁺ is used.

The melting temperature is $T_m = 71.5^\circ\text{C}$ close to the found one in 24. Furthermore, $\Delta H = 151.2\text{ kcal/mol}$ and $\Delta S = 444.7\text{ cal/mol/K}$. It is in the same range as the one found for in Fig 20 and 21.

With a wider view, we can also conclude that these thermodynamics parameters have only a slight change between LOOP4 and LOOP16.

5 Analysis of titrations - ITC

Isothermal titration calorimetry (ITC) is another method to assess the thermodynamic behavior of a reaction in solution.

The first plot is related to the raw data of ITC in Fig. 29. The expected behavior is observed, a decrease of the total power delivered after each injection due to the hybridization of both DNA strands until it finally saturates.

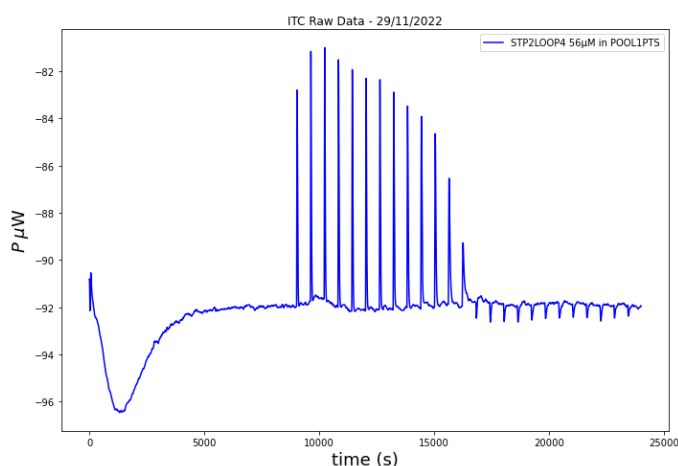


Figure 29: Raw Data for ITC - 29/11/2022

The amount of power used after each injection as a function of time is plotted in Fig. 30.

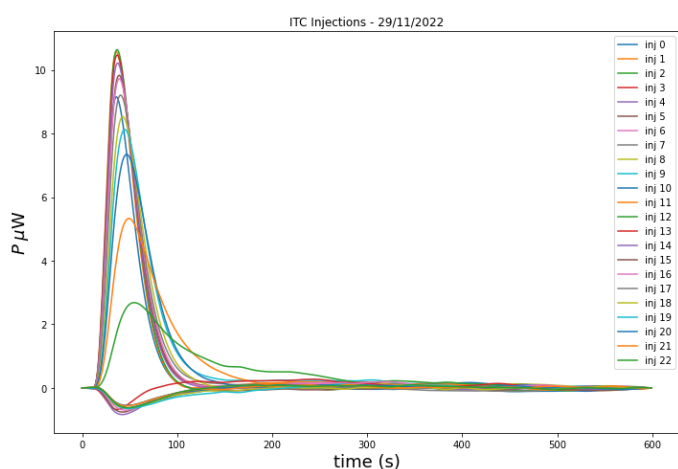


Figure 30: ITC Injections - 29/11/2022

The integration of power with respect to time can be used to calculate the reaction energy after each injection. The ITC experiment can also be used to determine the binding constant of the chemical reaction. The reaction

that we observe is similar to $A + B \rightarrow AB$, with a ligand and an analyte. A behavior like the one in Fig. 31 should be observed [18] (replacing ligand and analyte with Seq. 1 and Seq. 2).

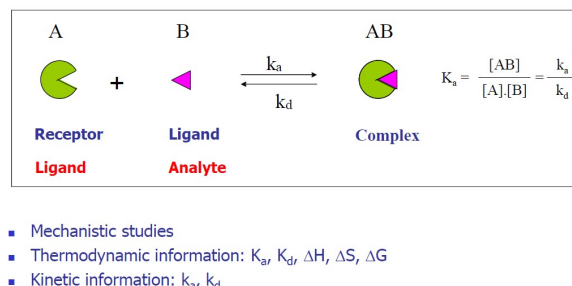


Figure 31: Hybridization reaction with the thermodynamic constants. Adapted from [18].

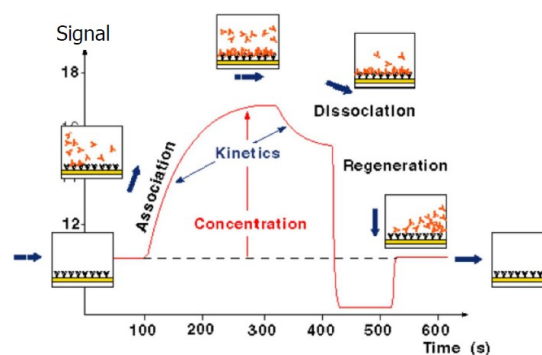


Figure 32: Response over time of the association followed by the dissociation. Adapted from [18].

With the strand titrations, evaluation of the reaction enthalpy can be done. On the other hand, the evaluation of the binding constants is more complex [2]. We can evaluate the binding constant with a model such as the one represented in Fig. 32 using a surface plasmon resonance technique. When the concentration of ligand is plotted versus the observed rate constant, the concentration at which half of the saturation is reached is the dissociation constant. In ITC, the evaluation of the binding constants is more complicated as the experiment is too short for the correct observation of the kinetic information. A solution might be to widen the plot to have a closer observation at its behaviour.

While being able to set the experimental temperature is one of the strengths of ITC relative to thermal melting analysis like DSC, it can be a weaknesses if some factors are not considered. One has to do with residual structure. When DNA hybridization or folding is studied by thermal melting, the unbound form is a high-temperature state whereas the structured form is the low-temperature state. ITC, on the other hand, is an isothermal measurement so both the bound and free states are at modest temperature and that means that the uncomplexed form may exhibit residual structure that can contribute to the measured heat and lead to complex temperature dependencies and nonlinear

behavior [16].

In addition, to obtain reliable binding constant (K_a) the concentrations of the interacting species have to be in a proper range. If the concentration of binding sites is much higher than $1/K_a$, all the ligand added will be bound until saturation. Otherwise, if it is below $1/K_a$, the binding isotherm is very shallow and full saturation is difficult to approach. For accurate values of K_a , the concentration of receptor binding sites should not be much higher than $1/K_a$. The dimensionless number obtained from multiplying K_a with the total binding site concentration is called the c -value. As a rule of thumb, c -values between 10 and 100 give good K_a -values. However, for very tight binding reactions, optimal concentrations are too small to yield measurable heat changes, and at the other extreme, when K_a is very low, the concentrations required for optimal c -values may be so high that aggregation can obscure the binding reaction [19].

The graph in Fig. 33 is obtained by a simple method. Each peak of Fig. 29 is integrated and the average of the last values is subtracted. With this graph, thermodynamic parameters can be obtained.

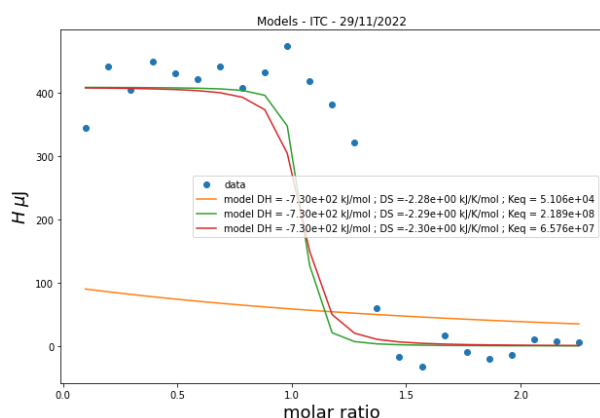


Figure 33: Models for ITC - 29/11/2022

This graph was used to corroborate if the reaction was complete and that the hybridization was smoothly. The molar ration was found to be 1:1. Furthermore, $\Delta H = 730 \text{ kJ/mol}$ or $\Delta H = 174 \text{ kcal/mol}$. In addition, $\Delta S = 2.29 \text{ kJ/K} \cdot \text{mol}$ or $\Delta S = 545 \text{ cal/K} \cdot \text{mol}$. It is relatively close to the value obtained either by DSC or with the web models (+/- 10 % similarity).

6 Conclusion

With this practical, the thermodynamic behavior of the hybridization of two complementary sequences was studied. We managed to understand how these techniques work, their limitations and how to analyze the data that is extracted from them. We found correlation between the results obtained by DSC, were compared with those from the Nupack and Dinamelt sites and ITC. The results showed similar trends especially concerning the molar enthalpy and the molar entropy. The DSC results were also compared with those from the experiment of a previous team that used a

LOOPSTP2L4 instead of LOOPSTP2L16. It was surprising to see a similar behavior, for example, for both the reaction temperature was around 70°C .

For the ITC, the concentrations of the DNA strands used were $10.1 \mu\text{M}$ for 1PTSPOOL and $63.3 \mu\text{M}$ for LOOPSTP2L16. A syringe containing $300 \mu\text{L}$ of LOOPSTP2L16 was delivered into 25 injections to a $1000 \mu\text{L}$ sample of 1PTSPOOL. The reaction was completed after 13 injections, which corresponds to 9.88 nmol of LOOPSTP2L16 that reacted with the 10.1 nmol of 1PTSPOOL (around a 1:1 molar ratio).

References

- [1] Ellen Sidransky, M.D: *Definition of hybridization*. National Human Genome Research Institute, 2022. <https://www.genome.gov/genetics-glossary/hybridization>.
- [2] Guillou, Hervé: *Laboratory report : Molecular interactions : nanocalorimetry of dna molecules*. Fall 2021.
- [3] Wikipedia, the free encyclopedia: *Holliday junction*. 2022. https://en.wikipedia.org/wiki/Holliday_junction.
- [4] Wikipedia, the free encyclopedia: *Genetic recombination*. 2022. https://en.wikipedia.org/wiki/Genetic_recombination.
- [5] Ortiz-Lombardía Miguel, González Ana, Eritja Ramón Aymamí Joan Azorín Fernando Coll Miquel: *Crystal structure of a dna holliday junction*. Nature Structural Biology, 1999. <https://doi.org/10.1038/13277>.
- [6] Lilley, David M. J.: *Structures of helical junctions in nucleic acids*. Quarterly Reviews of Biophysics, 33(2):109–159, 2000.
- [7] Geiselmann, Johannes: *Characterization of bio-molecular interactions - lecture booklet*. 2022.
- [8] M. E. Fornace, J. Huang, C. T. Newman N. J. Porubsky M. B. Pierce N. A. Pierce: *Nupack: analysis and design of nucleic acid structures, devices, and systems*. ChemRxiv, 2022. <https://nupack.org/home/references>.
- [9] Chikako Ragan, Michael Zuker, Mark A.Ragan: *Quantitative prediction of mirna-mrna interaction based on equilibrium concentrations*. PLoS Computational Biology, 2011. <http://www.unafold.org/Dinamelt/applications/hybridization-of-two-different-strands-of-dna-or-rna.php>.
- [10] Wikipedia, the free encyclopedia: *Differential scanning calorimetry*. 2022. https://en.wikipedia.org/wiki/Differential_scanning_calorimetry.
- [11] Guillou, Hervé: *Thermodynamics of molecular interactions, a practical hand-on using calorimetry and dna*. October 22, 2021.
- [12] Netzsch: *Functional principle of a heat-flux dsc*. 2022. <https://analyzing-testing.netzsch.com/fr/landingpages/principle-of-a-heat-flux-dsc>.
- [13] Bhadeshia, H. K. D. H.: *Introduction to differential scanning calorimetry*. University of Cambridge, Materials Science Metallurgy, 2002. <https://www.phase-trans.msm.cam.ac.uk/2002/Thermal2.pdf>.
- [14] Wikipedia, the free encyclopedia: *Isothermal titration calorimetry*. 2022. https://en.wikipedia.org/wiki/Isothermal_titration_calorimetry.
- [15] PCM, Wiki: *Dsc*. 2019. <https://thermalmaterials.org/wiki-pcm/dsc>.
- [16] Feng, A.: *Chapter 19 - studying rna-rna and rna-protein interactions by isothermal titration calorimetry*. 2009. <https://www.sciencedirect.com/science/article/abs/pii/S0076687909680198>.
- [17] AZoNetwork: *The working principle of isothermal titration calorimetry*. 2015. <https://www.azom.com/article.aspx?ArticleID=12258>.
- [18] Heyden, Angeline Van der: *Biomolecular interaction at interfaces*. 2022.
- [19] Jelesarov, I; Bosshard, H.: *Isothermal titration calorimetry and differential scanning calorimetry as complementary tools to investigate the energetics of biomolecular recognition*. 2009. <https://www.semanticscholar.org/paper/Isothermal-titration-calorimetry-and-differential-Jelesarov-Bosshard/ebd2714baf7cd8b0c03acf204f6b3a4239a7d01e>.